Novel Reconfigurable Full-Metal Cavity-Backed Slot Antennas Using Movable Metal Posts

Rui-Sen Chen, *Graduate Student Member, IEEE*, Lei Zhu, *Fellow, IEEE*, Sai-Wai Wong, *Senior Member, IEEE*, Xu-Zhou Yu, Yin Li, *Member, IEEE*, Wei He, Long Zhang, *Member, IEEE*, and Yejun He, *Senior Member, IEEE*

***Abstract*— Novel design concept of reconfigurable full-metal cavity-backed slot antennas (CBSAs) using movable metal posts is proposed in this article. It is found that the cavity mode with purely directional electric field is only affected by the metal post to be placed in parallel to its electric field. Thus, two orthogonal cavity modes TE_{101} and TE_{011} can be perturbed by two respective metal posts so as to independently tune the resonant frequencies of these two modes. Electromagnetic energy of the cavity modes can be radiated out through the slots on the top wall of the cavity. In this context, reconfigurable slot antennas with different functionalities, such as single-band, dual-band, dual-mode wideband, the tunable frequency with constant bandwidth, and tunable bandwidth with constant frequency, are thus constituted to demonstrate its attractive design feasibility. The frequency-reconfigurable cavity-back slot antenna with movable metal posts is proposed for the first time. The utilization of the metal posts allows us to achieve a continuous frequency tuning property, while the full-metal structure of the proposed antenna holds a high power-handling capacity and a high radiation efficiency. In final, a prototype of the dual-mode wideband slot antenna is designed, fabricated, and tested to reveal its total efficiency higher than 88% and stable radiation pattern over the tuning band. Good agreement between the measured and the simulated results well validates the presented design concept.**

***Index Terms*— Cavity-backed slot antenna (CBSA), full-metal, independent tuning, movable metal posts, reconfigurable antenna.**

I. Introduction

RECONFIGURABLE microwave circuits and antennas have been attracting much attention nowadays in the development of various modern communication systems, due to their attractive performances with varying and multiple frequency bands of operation. Among them, a reconfigurable antenna is highly demanded for transmitting and receiving wireless signal in these systems. For this purpose, a variety of reconfigurable antennas have been extensively designed and implemented on planar structure via the utilization of electronically controlled devices, such as microstrip antennas [1]–[6] and SIW slot antennas [7]–[9]. In [4], varactor diodes were utilized to bridge two portions of a patch antenna, by biasing the dc voltage of the diodes, tunable loading capacitance and tunable operating frequency were obtained. In [9], the switches were used to bridge the radiation-produced crossed-slots of the SIW cavity antenna, the OFF-state or ON-state of the switches could be selected to change the length of the slots, and thus achieved the agilities of frequency, polarization, and radiation pattern.

However, these reconfigurable antennas based on the electronic device often suffer from low power-handling capacity, low radiation efficiency, and high noise behaviors. Recently, the reconfigurable antennas based on dielectric fluids [10]–[14] and liquid metal [15]–[18] were researched and proposed to partly overcome these issues. The loading of dielectric fluids could adjust the effective dielectric constant to produce a frequency shift, while the liquid metal physically could modify the entire antenna structure as a parasitic element. Therefore, the performances of the antenna, such as operating frequency, polarization, and radiation pattern could be properly changed. In [12], the transformer oil was injected into the container below the patch antenna to obtain a tunable operating frequency. In [15], the liquid metal was injected to cover the slots on the patch to modify the effective size of the patch modes TM_{10} and TM_{30}, thereby causing a frequency shift. Herein, the injection of dielectric fluid and liquid metal could be controlled by using syringes or micropump to obtain a pressure difference.

Consider the fact that the aforementioned reconfigurable antennas on planar structure often suffer from relatively low power-handling capacity and relatively low efficiency, the metal cavity slot antennas have been widely developed as an alternative candidate. In [19], a tunable evanescent-mode cavity slot antenna using electronically controlled piezo disk was reported, the tunable frequency was obtained by changing the micro gap between the cavity post and the piezo disk. However, this method suffers from the sensitive fabrication of the micro gap, which may reduce the power-handling capacity.

Manuscript received October 18, 2020; revised January 18, 2021; accepted February 12, 2021. Date of publication April 5, 2021; date of current version October 6, 2021. This work was supported in part by the Shenzhen Science and Technology Program under Grant JCYJ20180305124543176 and Grant JCYJ20190728151457763, in part by the Natural Science Foundation of Guangdong Province under Grant 2018A030313481, in part by the Shenzhen University Research Startup Project of New Staff under Grant 860–000002110311, and in part by the National Natural Science Foundation of China under Grant 62071306. *(Corresponding author: Sai-Wai Wong.)*

Rui-Sen Chen is with the College of Electronics and Information Engineering, Shenzhen University, Shenzhen 518060, China, and also with the Department of Electrical and Computer Engineering, Faculty of Science and Technology, University of Macau, Macau 999078, China.

Lei Zhu is with the Department of Electrical and Computer Engineering, Faculty of Science and Technology, University of Macau, Macau 999078, China.

Sai-Wai Wong, Xu-Zhou Yu, Yin Li, Wei He, Long Zhang, and Yejun He are with the College of Electronics and Information Engineering, Shenzhen University, Shenzhen 518060, China (e-mail: wongsaiwai@ieee.org).

Color versions of one or more figures in this article are available at https://doi.org/10.1109/TAP.2021.3069584.

Digital Object Identifier 10.1109/TAP.2021.3069584

In this aspect, the metallic tuning screws or posts have been used to design tunable microwave filters [20], [21] and antennas [22]–[25]. The antennas in [22]–[25] focused on the reconfiguration of radiation pattern and polarization. In [25], the tuning screws were inserted into the waveguide-based power dividers to obtain a phase change of the transmitted signal, and the steering beam was thus obtained. However, as far as the authors know, the frequency-reconfigurable full-metal cavity slot antenna based on the metallic tuning screws has not been reported so far, which is our main focus in this presented work.

In this article, a novel class of reconfigurable full-metal cavity-backed slot antennas backed by the cavity with movable metal posts is proposed. The metal post can be moved to bring out perturbation on the cavity modes, and thus produce a frequency shift as desired. Next, two orthogonal cavity modes TE_{101} and TE_{011} are independently tuned by moving two respective metal posts, which are parallel to their own electric fields. Thus, single-band, dual-band, dual-mode wideband reconfigurable antennas are realized using this design method. A dual-mode wideband antenna prototype is finally fabricated and tested to demonstrate its attractive features in tuning the center frequency with constant bandwidth and the bandwidth with constant center frequency. Good agreement between the simulated and measured results is achieved in the interested band of operation, thus validating the proposed design concept.

II. Reconfigurable Cavity-Backed Slot Antennas

A. Reconfigurable Single-Band Antenna

Fig. 1 depicts the physical structure of the reconfigurable single-band cavity-backed slot antenna to be presented. It is composed of a resonant cavity with a radiation slot and a feeding slot, a coaxial-to-waveguide transition formed by a feeding cavity and an SMA port with an extended probe, and a loaded metal post on the side wall. The coaxial-to-waveguide transition is used to excite the desired cavity mode through the feeding slot. The feeding slot introduces an electric field along y-axis, namely, E_y, and then excites the cavity mode TE_{101} whose electric field is along the y-axis. Besides, the radiation slot is set across the E_y so as to radiate the energy of TE_{101} mode. The metal post is set along the y-axis to bring out proper perturbation on the TE_{101} mode toward frequency shift.

Fig. 2 shows the simulated $|S_{11}|$ without and with the loaded metal post. It can be seen that the resonant frequency of the TE_{101} shifts to a lower frequency by virtue of the metal post. To clearly provide an insight into the effect of the metal post, the electric and magnetic field distributions at two frequencies are provided in Fig. 3. Fig. 3(a) and (b) indicates that the electric field (E-field) is purely along the y-axis and the magnetic field (H-field) is in a loop at the xz plane with a null in the middle part. As the metal post is introduced, the electric field is still along the y-axis with a small inflection around the metal post, while the magnetic field in the middle part becomes stronger, as shown in Fig. 3(c) and (d). This means that the metal post hardly affects the electric field, but arouses a large effect on the magnetic field. Thus, the metal post brings out an inductive loading on the TE_{101} mode.

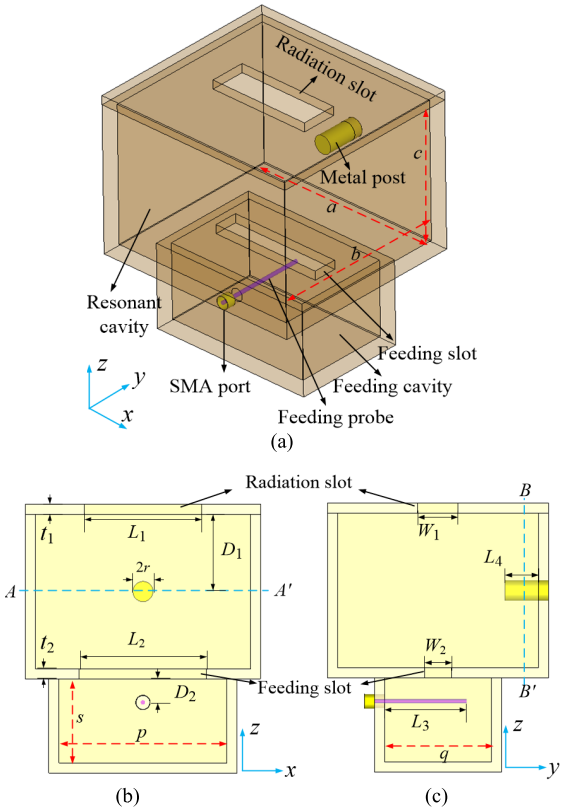

Fig. 1. Proposed reconfigurable cavity-backed slot antenna using movable metal post. (a) 3-D view. (b) Side view at xz plane. (c) Side view at yz plane.

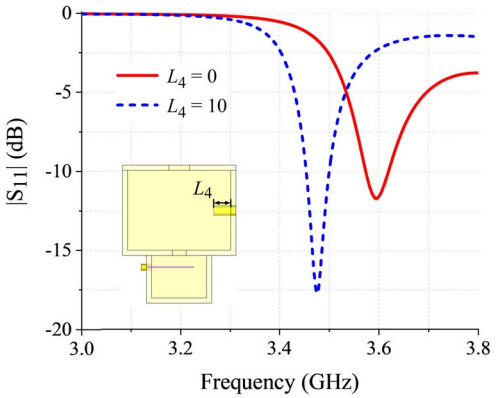

Fig. 2. Simulated $|S_{11}|$ with different lengths of the metal post. Dimensions (Unit: mm): $a = 64$, $b = 60$, $c = 46$, $p = 50$, $q = 32$, $s = 25$, $L_1 = 35$, $W_1 = 12$, $L_2 = 38$, $W_2 = 8$, $L_3 = 24.5$, $D_1 = 23$, $D_2 = 7$, $r = 3$, $t_1 = 5$, $t_2 = 3$.

Note that the metal post is open-circuited at one end and short-circuited at the other end.

Based on the previous work [27], the whole equivalent circuit model of the proposed reconfigurable slot antenna can be easily established and shown in Fig. 4. The C_{r1} and L_{r1} represent the LC-resonator model of the original TE_{101} mode, C_{f1} and C_{s1} represent the capacitive loadings of the feeding slot and radiation slot, respectively. The L_{p1} represents the inductive loading of the metal post. As illustrated in Fig. 4, the resonant frequency of TE_{101} mode can be calculated using (1). Here, the L_{p1} is treated as a tunable parameter, and the tunable L_{p1} is obtained by adjusting the length of the metal

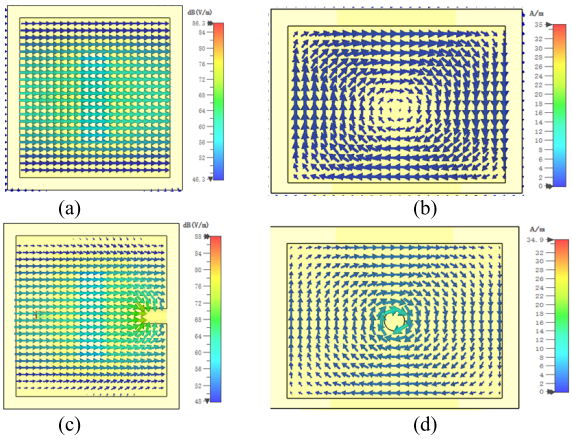

Fig. 3. Field distribution (E-field at A-A' plane and H-field at B-B' plane). (a) and (b) E-field and H-field at 3.595 GHz for $L_4 = 0$. (c) and (d) E-field and H-field at 3.477 GHz for $L_4 = 10$ mm.

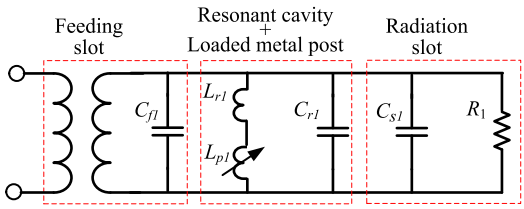

Fig. 4. Equivalent circuit model of the proposed reconfigurable slot antenna.

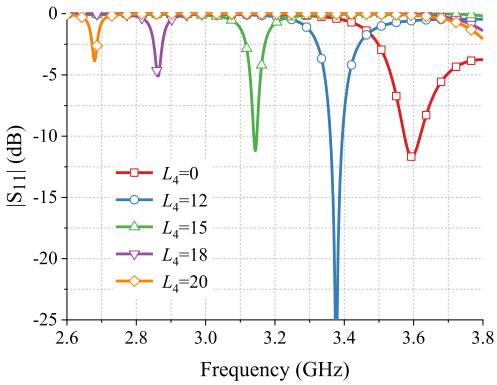

Fig. 5. Tunable frequency versus the length of the metal post.

post, such that one can deduce its tunable frequency of f_1 as

$$f_1 = \frac{1}{2\pi\sqrt{(L_{r1}+L_{p1})(C_{r1}+C_{f1}+C_{s1})}}. \quad (1)$$

Fig. 5 shows the resonant frequency of the TE_{101} under varying length (L_4) of the metal post. The increasing length of metal post increases the inductive loading parameter, i.e., inductance L_{p1}, resulting in the lower resonant frequency of the TE_{101} from 3.61 to 2.68 GHz as L_4 increases from 0 to 20 mm. Thus, the proposed approach exhibits its good feasibility in the design of reconfigurable cavity-backed slot antenna.

The increment of frequency shift mainly depends on the loaded inductance. Except for the length of the metal post, its radius and offset also affect the frequency shift, as illustrated in Fig. 6. A larger radius of the metal post produces a larger loaded inductance, and consequently produces a larger

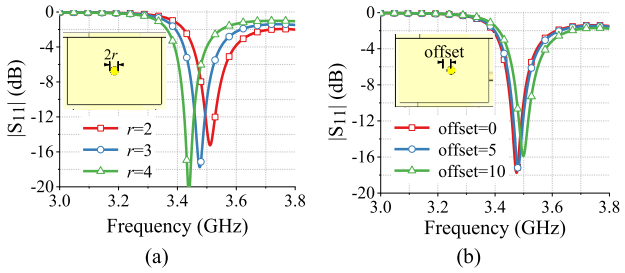

Fig. 6. Effects of (a) radius and (b) offset of the metal post.

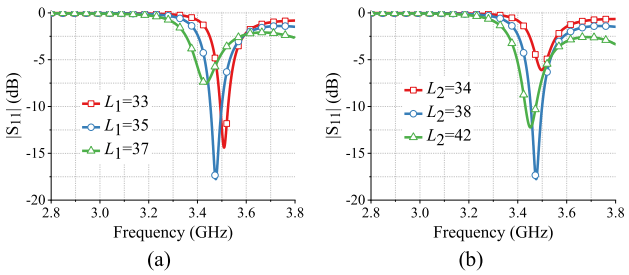

Fig. 7. Effects of radiation slot and feeding slot on the resonant frequencies. (a) Length of the radiation slot, L_1. (a) Length of the feeding slot, L_2.

frequency shift, as indicated in Fig. 6(a). Fig. 6(b) shows that a larger offset produces a little smaller frequency shift, which means that the metal post placed at the center of axis can produce the largest perturbation.

The increasing size of the radiation slot and the feeding slot produces an increasing capacitance loadings C_{s1} and C_{f1}, which results in a decreasing resonant frequency f_1 according to (1). Here, the effects of the lengths of the radiation slot and the feeding slot are discussed, as shown in Fig. 7. It can be seen that the increasing length of the slots causes a decreasing resonant frequency as predicted.

Then, a reconfigurable single-band cavity-backed slot antenna is designed. In practical implementation, impedance matching is a main factor to influence the tuning range. In this antenna, good impedance matching and realizable tuning range are achieved by using the trial-and-error method. After that, the final simulated result of the single-band antenna is obtained and shown in Fig. 8. The realizable tuning range with 10-dB return loss is from 3.6 to 3.14 GHz, and the tuning percentage in frequency as defined in (2) is calculated as 13.6%. f_H and f_L are the highest and lowest center frequencies, respectively. The radiation patterns are shown in Fig. 9, which demonstrates a stable radiation pattern in the tuning range

$$\eta = \frac{f_H - f_L}{(f_H + f_L)/2} \times 100\%. \quad (2)$$

B. Reconfigurable Dual-Band Antenna

As studied in the above section, it can be understood that the cavity mode is affected by the loaded metal post to be placed in parallel to the electric field, where the metal post and the electric field of TE_{101} mode are both along the y-axis. In a rectangular-waveguide cavity, there is another cavity mode with purely directional electric field distribution, i.e., TE_{011} mode, whose electric field is along x-axis.

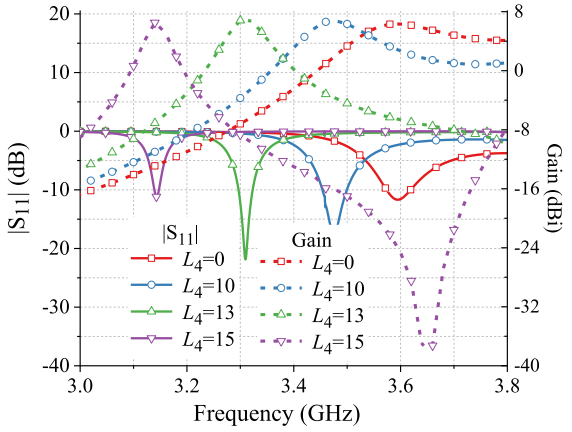

Fig. 8. Final simulated results of the reconfigurable single-band slot antenna. $a = 64$, $b = 60$, $c = 46$, $p = 50$, $q = 32$, $s = 25$, $L_1 = 35$, $W_1 = 12$, $L_2 = 38$, $W_2 = 8$, $L_3 = 24.5$, $D_1 = 23$, $D_2 = 7$, $r = 3$, $t_1 = 5$, $t_2 = 3$.

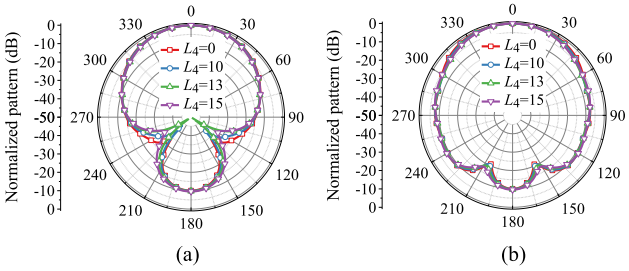

Fig. 9. Simulated radiation patterns of single-band reconfigurable antenna. (a) Radiation pattern at xz plane. (b) Radiation pattern at yz plane.

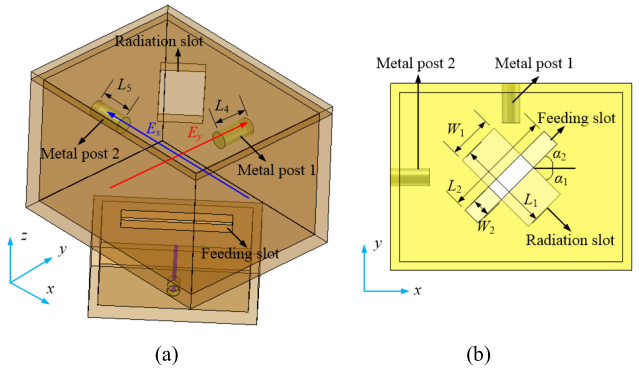

Fig. 10. Proposed reconfigurable dual-band cavity-backed slot antenna. (a) 3-D view. (b) Top view.

These two modes can be possibly used to design a dual-band slot antenna. As discussed previously, a reconfigurable dual-band slot antenna can be formed up by introducing two metal posts along x-axis and y-axis, respectively, as shown in Fig. 10. The feeding slot and radiation slot are both rotated to simultaneously excite the TE_{101} and TE_{011} modes for radiation. Here, the rotation angle of the radiation slot is set as $-45°$ (or $+45°$) to maintain the E- and H-plane radiation patterns at $-45°$ and $+45°$, while that of the feeding slot is finally determined after optimization.

The simulated $|S_{11}|$ of the dual-band antenna without the effect of the metal posts is shown in Fig. 11(a). The electric

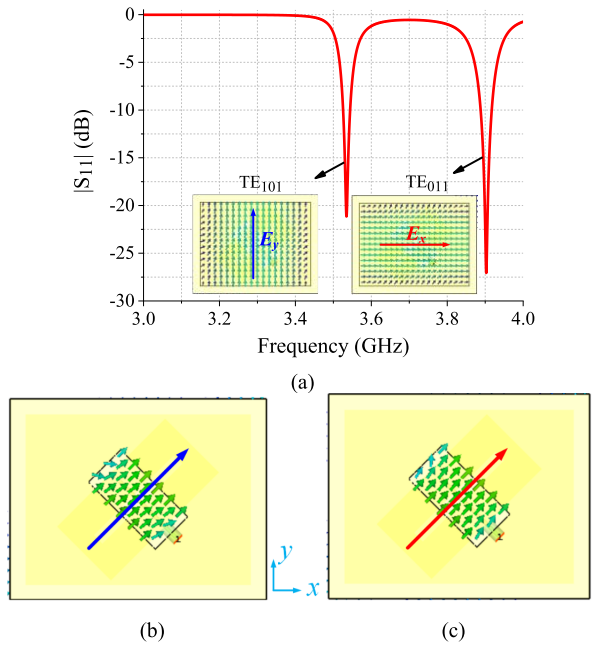

Fig. 11. (a) Simulated $|S_{11}|$ and modes' electric field distributions inside the cavity. (b) Electric field distribution at the radiation slot of TE_{101} mode at 3.553 GHz. (c) Electric field distribution at the radiation slot of TE_{011} mode at 3.876 GHz.

field distribution of the two resonant modes inside the cavity is also shown in this figure. It can be seen that the first mode is TE_{101} and the second mode is TE_{011}. It seems that they will have orthogonal polarization. However, in fact, these two modes can only radiate through the same radiation slot. The rotated radiation slot can simultaneously radiate the two modes. The electric field distributions of the two modes at the radiation slot are shown in Fig. 11(b) and (c), respectively. It can be seen that they have the same direction of the electric field. As the electric field at the radiation slot dominates the far-field radiation characteristic, these two modes have the same polarization of the radiation pattern.

Although the feeding and radiation slots affect the two modes at the same time, they produce different degrees of perturbations on these two modes. Besides, the metal post 1 (MP-1) along the y-axis only affects the TE_{101} mode, while the metal post 2 (MP-2) along the x-axis only affects the TE_{011} mode. According to the similar analysis, as described above, the equivalent circuit model of the reconfigurable dual-band antenna can be established and given in Fig. 12. For simplifying our analysis herein, each mode corresponds to a branch. The resonant frequency of TE_{101} mode is expressed as (1). Similarly, the resonant frequency of TE_{011} mode is given as the following:

$$f_2 = \frac{1}{2\pi\sqrt{(L_{r2} + L_{p2})(C_{r2} + C_{f2} + C_{s2})}}. \tag{3}$$

According to (1) and (3), the resonant frequencies of modes TE_{101} and TE_{011} can be independently tuned by modifying the inductances L_{p1} and L_{p2}. Here, the loaded inductances of L_{p1} and L_{p2} are dominated by the lengths of MP-1 (L_4) and MP-2 (L_5), respectively. To prove the independent tuning functionality of the two modes by virtue of the two metal

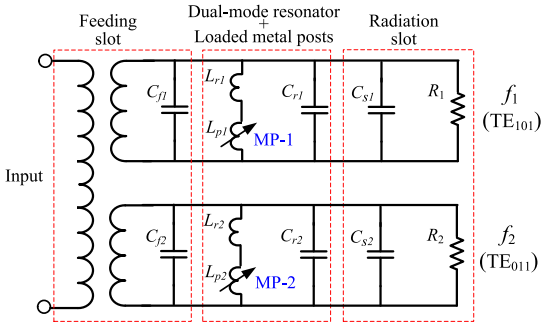

Fig. 12. Equivalent circuit model of the reconfigurable dual-band slot antenna (MP: metal post).

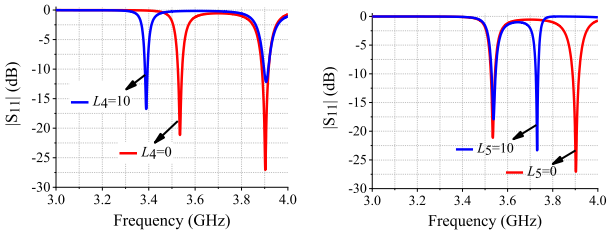

Fig. 13. Simulated $|S_{11}|$ with different lengths of the metal posts. (a) Length of metal post 1, L4. (b) Length of metal post 2, L5.

posts, the resonant frequencies of the two modes under varying L_4 and L_5 are shown in Fig. 13. It can be seen that both of these two modes can be indeed independently tuned without affecting the other mode. As a convenient way to understand the mechanism of independent tuning, the cavity mode with purely directional electric field distribution is only determined by the metal post to be placed in parallel to its electric field.

As such, a reconfigurable dual-band cavity-backed slot antenna is presented and designed. The final simulated results are shown in Fig. 14. The tunable length of the movable metal post 1 produces a tunable frequency of the first band, and slightly affects the second band. The tuning range of the first band with 10-dB return loss is from 3.56 to 3.15 GHz with a tuning percentage of 11.5%. Meanwhile, the tunable length of the metal post 2 produces a tunable frequency of the second band, and slightly affects the first band. The tuning range of the second band with 10-dB return loss is from 3.88 to 3.23 GHz with a tuning percentage of 18.3%. It can be also seen that the tuning frequency of the second band is changed across the first band, as shown in Fig. 14(c) and (d), which well demonstrates a stable operation of the proposed reconfigurable slot antenna based on the cavity modes. The radiation patterns of the reconfigurable dual-band antenna in the tuning range are shown in Fig. 15, which also indicate that the reconfigurable dual-band antenna has a stable radiation pattern.

III. Reconfigurable Wideband Slot Antennas

In the above section, two reconfigurable cavity-backed slot antennas with single- and dual-band functionality are presented under single-mode operation. In this section, an alternative reconfigurable wideband slot antenna will be designed under dual-mode operation. The geometry of the proposed dual-band antenna is depicted in Fig. 10, where the two modes

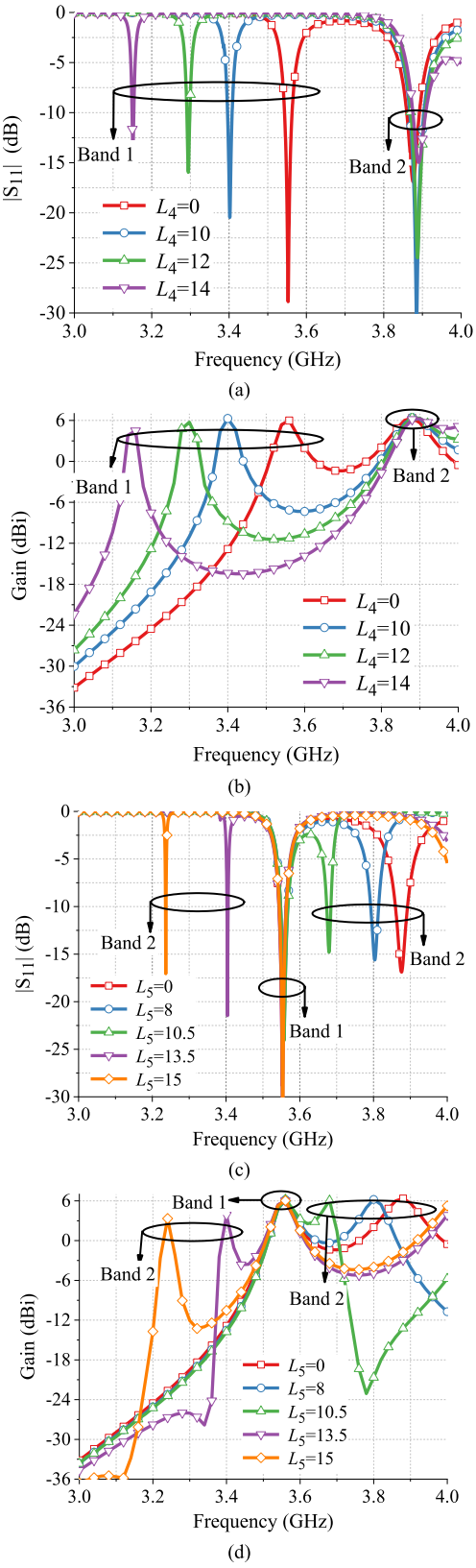

Fig. 14. Final simulated results of the reconfigurable dual-band antenna. (a) $|S_{11}|$ and (b) realized gain under varying length of metal post 1, L_4. (c) $|S_{11}|$ and (d) realized gain under varying length of metal post 2, L_5. Dimensions (Unit: mm): $a = 74$, $b = 56$, $c = 48$, $p = 50$, $q = 25$, $s = 25$, $L_1 = 31$, $W_1 = 15$, $L_2 = 37$, $W_2 = 4$, $L_3 = 21$, $D_1 = 23$, $D_2 = 14$, $r = 3$, $t_1 = 5$, $t_2 = 3$, $\alpha_1 = 45°$, $\alpha_2 = 45°$.

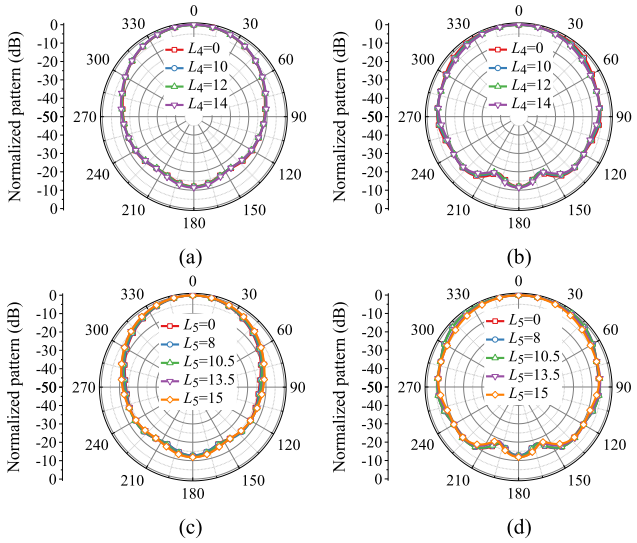

Fig. 15. Simulated radiation patterns of dual-band reconfigurable antenna at (a) *xz*-plane of band 1, (b) *yz* plane of band 1, (c) *xz* plane of band 2, and (d) *yz* plane of band 2.

can be resonated in the same band so as to form a dual-mode wide operating band due to the disappearance of radiation null between the two resonant frequencies. In other words, the configuration of this antenna is basically the same as that of the above-discussed reconfigurable dual-band antenna, but they have distinct physical dimensions. Fig. 16 shows the simulated results of such a dual-mode wideband slot antenna. The dual-mode slot antenna based on TE_{101} and TE_{011} modes has been reported in [26], so the similar description on the proposed dual-mode antenna is not repeated here. The main target in this work is to design a reconfigurable wideband cavity-backed slot antenna based on these two modes and the movable metal posts.

Here, the bandwidth (*BW*) of the dual-mode antenna is approximately given in as the frequency difference between f_1 (TE_{101} mode) and f_2 (TE_{011} mode). Meanwhile, the fractional bandwidth (*FBW*) is defined as the ratio of BW/f_c, where f_c represents the center frequency of the operating band. As shown in (1) and (3), f_1 and f_2 can be independently modified in such a way that the *BW*, *FBW*, and f_c can be all flexibly controllable.

Basically speaking, the *BW* can be hardly controlled by using the conventional reconfiguration technique, since the resonant frequencies of these modes are unable to be independently controlled. Fortunately, the two modes of the proposed antenna can be independently adjusted by modifying their respective metal posts, as shown in Fig. 14. This attractive property can be effectively applied to design a frequency-reconfigurable slot antenna with constant *FBW* and bandwidth-reconfigurable slot antenna with constant center frequency.

A. Frequency-Reconfigurable Antenna with Constant FBW

Let us start to design the frequency-reconfigurable cavity-backed slot antenna with constant *FBW* at first. As f_1 and f_2 are tuned by modifying the lengths of the metal posts, all the

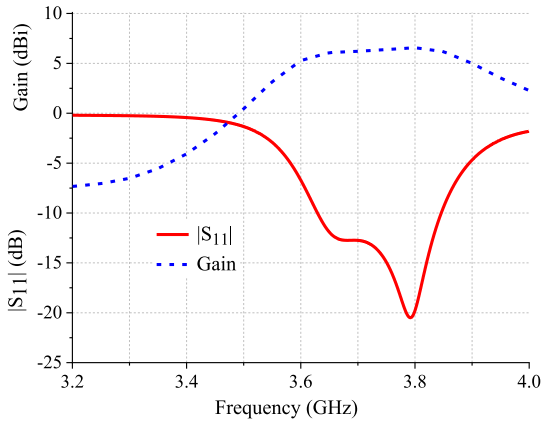

Fig. 16. Initial performance of the wideband dual-mode antenna. Dimensions (Unit: mm): $a = 80$, $b = 66$, $c = 51$, $p = 52$, $q = 25$, $s = 25$, $L_1 = 42$, $W_1 = 10$, $L_2 = 52$, $W_2 = 12$, $L_3 = 18$, $D_1 = 26$, $D_2 = 6$, $r = 3$, $t_1 = 3$, $t_2 = 3$, $\alpha_1 = 45°$, $\alpha_2 = 60°$. Lengths of metal post 1 and metal post 2 are both equal to 0.

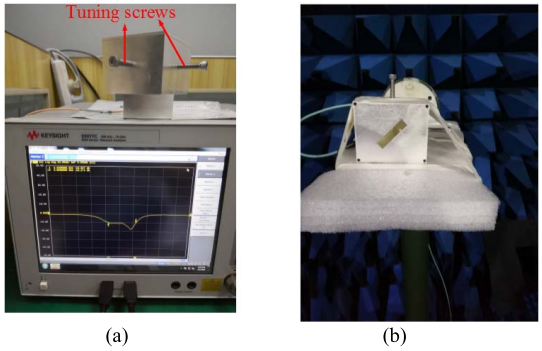

Fig. 17. Photographs of experimental set-up for testing the proposed antenna. (a) S-parameter. (b) Far-zone radiation.

BW, *FBW*, and f_c can be operated as a function of L_4 and L_5 (starting from an initially obtained antenna performance, as shown in Fig. 16). Here, the *FBW* is given by the initial performance, for example, the *FBW* of the antenna shown in Fig.16 is 5.8%. The f_c is the targeted center frequency during the frequency tuning. Once the *FBW* and the f_c are given, the targeted reconfigurable frequencies f_1 and f_2 can be determined by using (4), and the specified f_1 and f_2 can be obtained by properly tuning the lengths of the two metal posts

$$\left.\begin{aligned} f_2 + f_1 &= 2 \cdot f_c \\ f_2 - f_1 &= FBW \cdot f_c \end{aligned}\right\}. \tag{4}$$

For proof-of-concept, an antenna prototype is fabricated and tested after our design. The experimental set-up photographs for S-parameter and far-zone radiation are provided in Fig. 17(a) and (b), respectively. Two tuning metal screws are used as the tuning elements and the tuning process is executed by twisting the metal screws. The measured and simulated $|S_{11}|$, realized gain, and total efficiency are illustrated in Fig. 18. Three states are presented to show the tunable center frequency with a constant *FBW* of 5.8%. The lengths of the two metal posts and the simulated/measured results at these three states are provided in Table I. The tuning

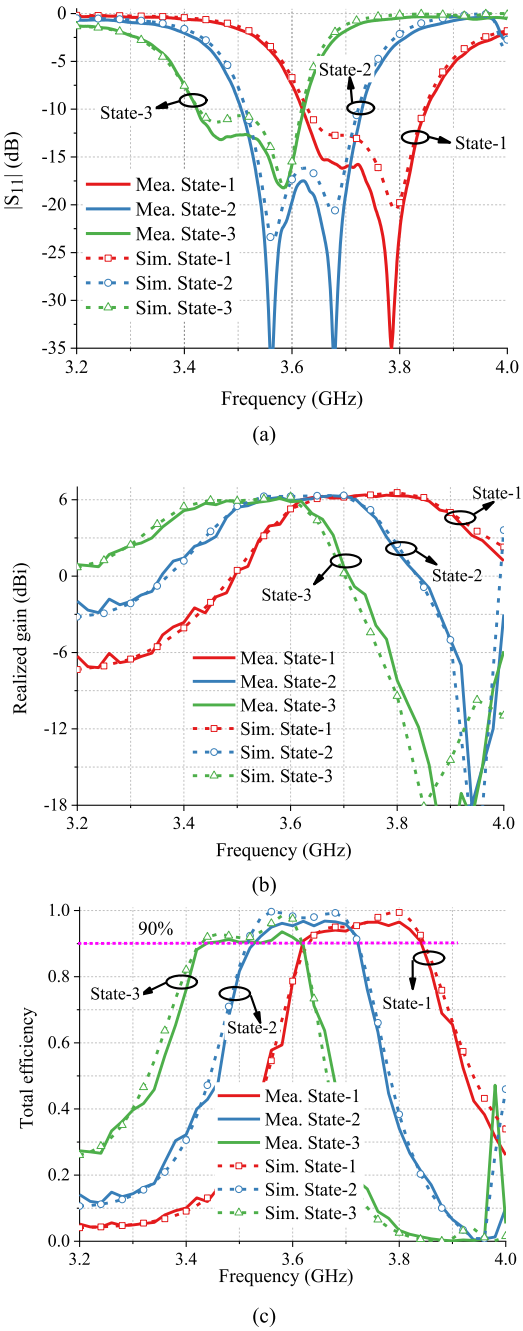

Fig. 18. Simulated and measured results with different states of movable metal posts for tunable frequency. (a) $|S_{11}|$. (b) Realized gain. (c) Total efficiency.

range of the wideband slot antenna is from 3.735 to 3.5GHz with a 10-dB return loss, and the tuning percentage is about 6.5%. The measured total efficiencies of the antenna at these three states are all higher than 88%, while the simulated ones are higher than 90%. The simulated and measured radiation patterns at the center frequencies of the three states are shown in Fig. 19. The co-polarizations of them at these three states are almost unchanged, which demonstrates a stable radiation pattern. The cross-polarizations are better than 20dB. Good agreement between simulated and measured results is satisfactorily achieved.

TABLE I

RESULTS OF FREQUENCY-RECONFIGURABLE ANTENNA WITH CONSTANT FBW

States	Case	L_4 (mm)	L_5 (mm)	Results				
				f_c (MHz)	BW (MHz)	FBW	PG (dBi)	TE (peak)
State-1	Mea.	0	0	3735	230	6%	6.4	>91% (96%)
	Sim.	0	0	3738	216	5.8%	6.6	>92% (99%)
State-2	Mea.	8.1	9.4	3620	218	6%	6.3	>90% (95%)
	Sim.	8.1	9.4	3620	210	5.8%	6.4	>91% (99%)
State-3	Mea.	9.9	12.2	3500	204	5.8%	6.1	>88% (92%)
	Sim.	9.9	12.2	3498	203	5.8%	6.2	>90% (98%)

FBW: Fabrication bandwidth; PG: Peak Gain; TE: Total efficiency.

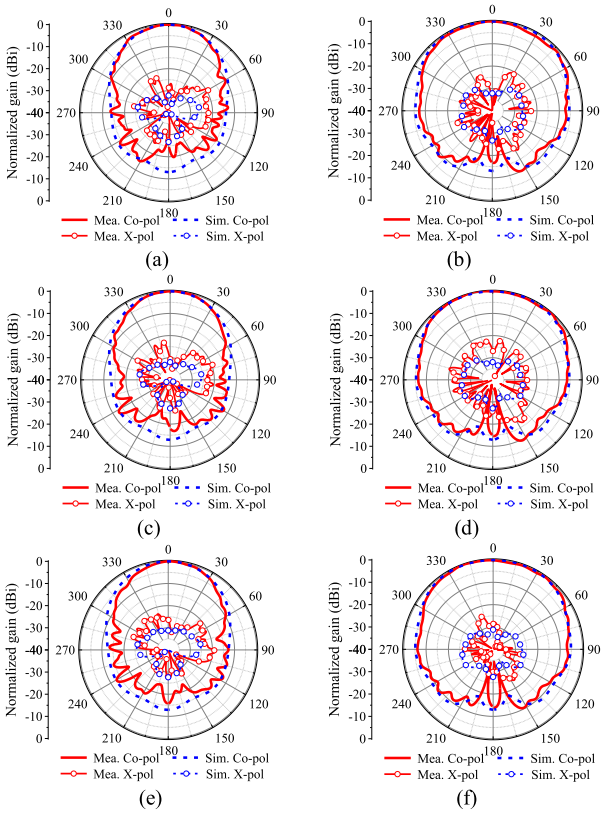

Fig. 19. Measured and simulated radiation patterns at E-plane and H-plane. (a) and (b) 3.735 GHz of State-I. (c) and (d) 3.62 GHz of State-II. (e) and (f) 3.5 GHz of State-III.

B. FBW-Reconfigurable Antenna with Constant Center Frequency

Next, the proposed design concept is further used to design a bandwidth-reconfigurable antenna with constant center frequency. In this design, the center frequency f_c is given, while the FBW is purposively set during the tuning process. According to (4), the specified frequencies f_1 and f_2 can be obtained by properly tuning the lengths of the two metal posts. In particular, a varying bandwidth is attained by twisting the two metal posts with opposite direction, i.e., increasing (or decreasing) the length of the metal post 1 (L_4) and decreasing (or increasing) the length of metal post 2 (L_5). Fig. 20 shows the simulated and measured $|S_{11}|$ of tunable operating bandwidth with a constant center frequency of 3.62 GHz. Good agreement between them is obtained over the frequency range. The measured bandwidth can be flexibly tuned in a range from

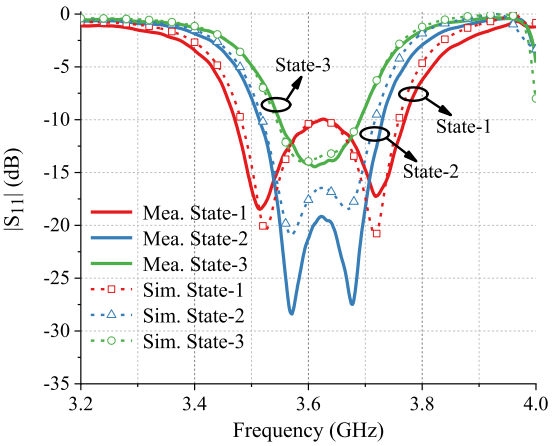

Fig. 20. Simulated and measured return loss with different states of the metal posts for tunable bandwidth.

TABLE II
RESULTS OF BANDWIDTH-RECONFIGURABLE ANTENNA WITH CONSTANT CENTER FREQUENCY

States	Case	L_4 (mm)	L_5 (mm)	Results		
				f_c (MHz)	*BW* (MHz)	*FBW*
State-1	Mea.	7.2	10.2	3620	294	8.1%
	Sim.	7.2	10.2	3620	280	7.8%
State-2	Mea.	8.2	9.3	3622	215	5.9%
	Sim.	8.2	9.3	3620	200	5.5%
State-3	Mea.	8.5	8.8	3620	142	4%
	Sim.	8.5	8.8	3620	145	4.1%

294 to 142 MHz with a 10-dB return loss. The detailed results are further provided in Table II. In fact, the BW or FBW can be made as small as possible by further increasing L_4 and decreasing L_5.

C. Comparison

The comparison with other reconfigurable antennas is provided in Table III. Here, we give a definition that the electronically controlled tuning elements have fast tuning speed, while the manually controlled tuning elements have slow tuning speed; The metal cavity has high power-handling capacity (the antenna [19] using the piezo disk as the tuning element, and has 80W power capacity, it is considered to have middle power-handling capacity), the planar antenna has low power-handling capacity as usual. The reliability is compared under the consideration of the long-term operation (requirement of power consumption will reduce the reliability in the long-term operation) and the effect of vibration (the utilization of liquid material and the electronic tuning elements result in a low reliability under the effect of vibration).

The comparisons in Table III reveal that the main disadvantage of the proposed reconfigurable antenna is the low tuning speed, which is commonly shared by many reported works using manually controlled tuning elements [12], [15], [18], [24], [25]. The cost of low tuning speed can bring out a low power loss and get a high antenna efficiency in return. Besides, compared to the frequency-reconfigurable antennas, i.e., except for [24] and [25], only the proposed antenna can realize dual-mode wideband antenna with reconfigurable frequency and bandwidth, while other antennas all operate in a narrow band under single-mode operation. In addition, the proposed reconfigurable antenna has high power-handling capacity and high long-term reliability.

D. Manufacturing Process

In the simulation model, the metal post is used as the perturbation method, and the length of metal post can be flexibly set. However, to obtain the tunable length of the metal post in the practical implementation, the metal post should be replaced by the tuning metal screws, as shown in Fig. 17. In this work, the antenna is fabricated using the computer numerical control (CNC) fabrication process. The whole antenna cannot be directly manufactured using the CNC process. In our fabrication, the antenna is divided into three parts, as shown in Fig. 21(a), and these three parts can be directly manufactured using the CNC process. Two screwed holes are set to place and twist the two tuning screws. One via hole in the feeding cavity is set to assemble the SMA connecter, as shown in Fig. 21(b).

IV. DISCUSSION

A. Design Methodology for Reconfigurable Slot Array

Antenna arrays are usually required to achieve higher gain. For conventional frequency-reconfigurable antenna arrays, each antenna unit requires one group of tuning elements. Thus, the reconfigurable antenna arrays will have quite a complicated antenna structure, but they can be indeed realized with the proper design. The proposed reconfigurable antenna is tuned by using the screws, it seems that it is hard to configure an antenna array. However, in contrast, the design of reconfigurable antenna array using the proposed design concept is easy. On one hand, our previous work [28] showed that multiple radiation slots could be placed on the top wall of an enlarged cavity to obtain an increasing gain, as all the radiation slots are directly fed by the electric field of the cavity modes. On the other hand, the metal posts are just employed to tune the resonant frequencies of the cavity modes. Thus, in the same way, multiple radiation slots can be placed on the top wall of the proposed reconfigurable antenna with an enlarged cavity, thus higher gain can be obtained and the reconfiguration property can be maintained.

B. Control Mechanism

The moveable metal posts in the simulation model are replaced by the tuning screws in the practical antenna. The metal screws are manually controlled in this measured prototype, as this measured prototype is presented to validate the proposed design concept. Good agreement between measured results and simulated results verifies the tuning capability with a prescribed accuracy. The proposed mechanism could also be electromechanically controlled by using servomotors to modify the penetration lengths of the tuning screws inside the cavity, which can be referred to [29]. This method will be able to increase the tuning speed.

C. Practical Application

The proposed reconfigurable antenna can be used as the base-station antenna for the application in the multiple-band

TABLE III
COMPARISONS WITH REPORTED RECONFIGURABLE ANTENNAS

Ref.	Structure	Tuning Mechanism	Reconfiguration capability	Band	Tuning range	Tuning speed	Total efficiency	Power capacity	Reliability
[2]	Microstrip	Varactors	Frequency	Dual band	31% / 22%	Fast	>50%	Low	Low
[9]	SIW slot	p-i-n Diodes	Frequency Polarization Radiation pattern	Single band	LP: 3.8% CP: 1.7%	Fast	>49%	Low	Low
[12]	Patch	Liquid dielectric	Frequency	Single band	24.7%	Slow	High: >87%	Low	Low
[15]	Patch	Liquid metal	Frequency	Dual band	10% / 30%	Slow	N.G.	Low	Low
[18]	Patch	Liquid metal	Frequency Polarization	Single band	LP: 11.6% CP: 24%	Slow	LP: >74% CP:> 43%	Low	Low
[19]	Metal cavity	Electronical piezo disk	Frequency	Single band	25%	Fast	High: >85%	Middle (80W)	Low
[24]	Metal cavity	Tuning screws	Radiation pattern	Single band	N.A.	Slow	High: >80%	High	High
[25]	Metal cavity	Tuning screws	Radiation pattern	Single band	N.A.	Slow	High: >90%	High	High
This work	Metal cavity	Tuning screws	Frequency Bandwidth	Single band Dual band Wideband	13.6% 11.5% / 18.3% 5.6%	Slow	High: >88%	High	High

LP: Linear polarization; CP: Circular polarization; N.A.: Not applicable; N.G.: Not given.

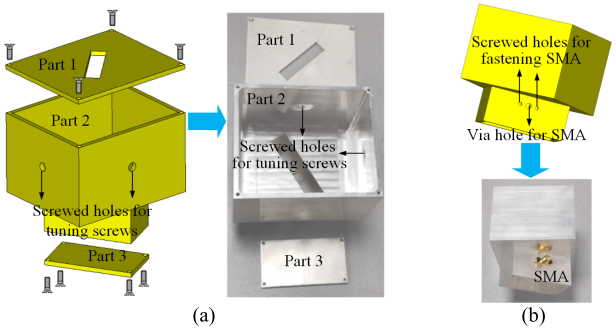

Fig. 21. Manufacturing process of the proposed antenna prototype. (a) Assembly of whole antenna. (b) Assembly of SMA port.

mobile communication systems, as this kind of system often requires high power-handling capacity for long-distance communication and high reliability for long-term operation. Besides, base-station antennas do not require fast tuning speed, as they usually work at a certain frequency for a relatively long term. Thus, they are only required that the frequency can be switched to other frequencies. The frequency-reconfigurable devices with fast tuning speed are usually applied to frequency-hopping communication system, or the systems with the required high anti-interference by quickly switching the operating frequencies, such as the radar communication system.

V. CONCLUSION

In this article, a novel design of reconfigurable full-metal cavity-backed slot antennas is presented and realized based on cavity modes and tuning posts. Benefited by the independent frequency tunings of the two orthogonal modes TE_{101} and TE_{011}, reconfigurable antennas with different functionalities can be effectively realized. An antenna prototype for measurement is presented to verify the design concept, which can indeed effectively achieve reconfigurations of operating frequency and operating bandwidth. Besides, the proposed reconfigurable antennas are exhibited to have their unique features in independent and continuous tuning capability, high power-handling capacity, low loss, high efficiency, unidirectional radiation, and stable radiation pattern. In addition, the effects of the metal post on the cavity modes and their relevant radiating energy via the slots are both employed to introduce extensive feasibility in the design of other reconfigurable waveguide-based slot antennas, such as reconfigurable dual-polarization slot antenna and reconfigurable cylindrical-waveguide slot antenna. Although the proposed reconfigurable antenna has a relatively slower tuning speed, it has low loss, high efficiency, high power-handling capacity, and high long-term reliability. These merits make the proposed reconfigurable antenna suitable for the application in multi-band mobile wireless communication system.

REFERENCES

[1] N. Nguyen-Trong, L. Hall, and C. Fumeaux, "A frequency- and polarization-reconfigurable stub-loaded microstrip patch antenna," *IEEE Trans. Antennas Propag.*, vol. 63, no. 11, pp. 5235–5240, Nov. 2015.

[2] N. Nguyen-Trong, A. Piotrowski, and C. Fumeaux, "A frequency-reconfigurable dual-band low-profile monopolar antenna," *IEEE Trans. Antennas Propag.*, vol. 65, no. 7, pp. 3336–3343, Jul. 2017.

[3] A. Boukarkar, X. Q. Lin, J. W. Yu, P. Mei, Y. Jiang, and Y. Q. Yu, "A highly integrated independently tunable triple-band patch antenna," *IEEE Antennas Wireless Propag. Lett.*, vol. 16, pp. 2216–2219, Aug. 2017.

[4] L. Ge, M. Li, J. Wang, and H. Gu, "Unidirectional dual-band stacked patch antenna with independent frequency reconfiguration," *IEEE Antennas Wireless Propag. Lett.*, vol. 16, pp. 113–116, Aug. 2017.

[5] M.-C. Tang, Z. Wen, H. Wang, M. Li, and R. W. Ziolkowski, "Compact, frequency-reconfigurable filtenna with sharply defined wideband and continuously tunable narrowband states," *IEEE Trans. Antennas Propag.*, vol. 65, no. 10, pp. 5026–5034, Oct. 2017.

[6] H. A. Majid, M. K. A. Rahim, M. R. Hamid, and M. F. Ismail, "A compact frequency-reconfigurable narrowband microstrip slot antenna," *IEEE Antennas Wireless Propag. Lett.*, vol. 11, pp. 616–619, Aug. 2012.

[7] F. Giuppi, A. Georgiadis, A. Collado, M. Bozzi, and L. Perregrini, "Tunable SIW cavity backed active antenna oscillator," *Electron. Lett.*, vol. 46, no. 15, pp. 1053–1055, Jul. 2010.

[8] A. Pourghorban Saghati and K. Entesari, "A reconfigurable SIW cavity-backed slot antenna with one octave tuning range," *IEEE Trans. Antennas Propag.*, vol. 61, no. 8, pp. 3937–3945, Aug. 2013.

[9] L. Ge, Y. Li, J. Wang, and C.-Y.-D. Sim, "A low-profile reconfigurable cavity-backed slot antenna with frequency, polarization, and radiation pattern agility," *IEEE Trans. Antennas Propag.*, vol. 65, no. 5, pp. 2182–2189, May 2017.

[10] M. Konca and P. A. Warr, "A frequency-reconfigurable antenna architecture using dielectric fluids," *IEEE Trans. Antennas Propag.*, vol. 63, no. 12, pp. 5280–5286, Dec. 2015.

[11] Y.-H. Qian and Q.-X. Chu, "A polarization-reconfigurable water-loaded microstrip antenna," *IEEE Antennas Wireless Propag. Lett.*, vol. 16, pp. 2179–2182, 2017.

[12] S. Wang, L. Zhu, and W. Wu, "A novel frequency-reconfigurable patch antenna using low-loss transformer oil," *IEEE Trans. Antennas Propag.*, vol. 65, no. 12, pp. 7316–7321, Dec. 2017.

[13] A. Singh, I. Goode, and C. E. Saavedra, "A multistate frequency reconfigurable monopole antenna using fluidic channels," *IEEE Antennas Wireless Propag. Lett.*, vol. 18, no. 5, pp. 856–860, May 2019.

[14] J. Kim and J. Oh, "Liquid-crystal-embedded aperture-coupled microstrip antenna for 5G applications," *IEEE Antennas Wireless Propag. Lett.*, vol. 19, no. 11, pp. 1958–1962, Nov. 2020.

[15] L. Song, W. Gao, C. O. Chui, and Y. Rahmat-Samii, "Wideband frequency reconfigurable patch antenna with switchable slots based on liquid metal and 3-D printed microfluidics," *IEEE Trans. Antennas Propag.*, vol. 67, no. 5, pp. 2886–2895, May 2019.

[16] L. Song, W. Gao, and Y. Rahmat-Samii, "3-D printed microfluidics channelizing liquid metal for multipolarization reconfigurable extended E-shaped patch antenna," *IEEE Trans. Antennas Propag.*, vol. 68, no. 10, pp. 6867–6878, Oct. 2020.

[17] C. Xu, Z. Wang, Y. Wang, P. Wang, and S. Gao, "A polarization-reconfigurable wideband high-gain antenna using liquid metal tuning," *IEEE Trans. Antennas Propag.*, vol. 68, no. 8, pp. 5835–5841, Aug. 2020.

[18] Y. Liu, Q. Wang, Y. Jia, and P. Zhu, "A frequency- and polarization-reconfigurable slot antenna using liquid metal," *IEEE Trans. Antennas Propag.*, vol. 68, no. 11, pp. 7630–7635, Nov. 2020.

[19] A. Semnani, M. D. Sinanis, and D. Peroulis, "An evanescent-mode cavity-backed high-power tunable slot antenna," *IEEE Trans. Antennas Propag.*, vol. 67, no. 6, pp. 3712–3719, Jun. 2019.

[20] S.-W. Wong, F. Deng, J.-Y. Lin, Y.-W. Wu, L. Zhu, and Q.-X. Chu, "An independently four-channel cavity diplexer with 1.1–2.8 GHz tunable range," *IEEE Microw. Wireless Compon. Lett.*, vol. 27, no. 8, pp. 709–711, Aug. 2017.

[21] S.-W. Wong *et al.*, "Individually frequency tunable dual- and triple-band filters in a single cavity," *IEEE Access*, vol. 5, pp. 11615–11625, Jul. 2017.

[22] J. A. Ruiz-Cruz, M. M. Fahmi, S. A. Fouladi, and R. R. Mansour, "Waveguide antenna feeders with integrated reconfigurable dual circular polarization," *IEEE Trans. Microw. Theory Techn.*, vol. 59, no. 12, pp. 3365–3374, Dec. 2011.

[23] P. Sanchez-Olivares and J. L. Masa-Campos, "Mechanically reconfigurable conformal array antenna fed by radial waveguide divider with tuning screws," *IEEE Trans. Antennas Propag.*, vol. 65, no. 9, pp. 4886–4890, Sep. 2017.

[24] P. Sanchez-Olivares, J. L. Masa-Campos, and J. Hernandez-Ortega, "Mechanical technique to customize a waveguide-slot radiating performance," *IEEE Trans. Antennas Propag.*, vol. 66, no. 1, pp. 426–431, Jan. 2018.

[25] P. Sanchez-Olivares, J. L. Masa-Campos, A. T. Muriel-Barrado, R. Villena-Medina, and G. M. Fernandez-Romero, "Mechanically reconfigurable linear array antenna fed by a tunable corporate waveguide network with tuning screws," *IEEE Antennas Wireless Propag. Lett.*, vol. 17, no. 8, pp. 1430–1434, Aug. 2018.

[26] Y.-M. Wu *et al.*, "Design of triple-band and triplex slot antenna using triple-mode cavity resonator," *IET Microw., Antennas Propag.*, vol. 13, no. 13, pp. 2303–2309, Jul. 2019.

[27] R.-S. Chen *et al.*, "High-isolation in-band full-duplex cavity-backed slot antennas in a single resonant cavity," *IEEE Trans. Antennas Propag.*, early access, Oct. 27, 2020, doi: 10.1109/TAP.2020.3032846.

[28] R.-S. Chen *et al.*, "High-efficiency and wideband dual-resonance full-metal cavity-backed slot antenna array," *IEEE Antennas Wireless Propag. Lett.*, vol. 19, no. 8, pp. 1360–1364, Aug. 2020.

[29] J. Zhou and J. Huang, "Intelligent tuning for microwave filters based on multi-kernel machine learning model," in *Proc. 5th IEEE Int. Symp. Microw., Antenna, Propag. EMC Technol. Wireless Commun.*, Oct. 2013, pp. 259–266.

Rui-Sen Chen (Graduate Student Member, IEEE) was born in Fujian, China. He received the B.S. degree from the Hunan University of Science and Technology, Hunan, China, in 2012, and the master's degree in electromagnetic field and radio technology from the South China University of Technology, Guangzhou, China, in 2015. He is currently pursuing the Ph.D. degree with the College of Electronics and Information Engineering, Shenzhen University, Shenzhen, China.

He was a Research Assistant with the Faculty of Science and Technology, University of Macau, Macau, China, from January 2020 to December 2020. His current research interests include microwave filter, antenna, and cavity components.

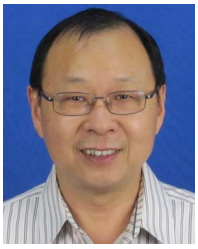

Lei Zhu (Fellow, IEEE) received the B.Eng. and M.Eng. degrees in radio engineering from the Southeast University, Nanjing, China, in 1985 and 1988, respectively, and the Ph.D. degree in electronic engineering from the University of Electro-Communications, Tokyo, Japan, in 1993.

From 1993 to 1996, he was a Research Engineer with Matsushita-Kotobuki Electronics Industries Ltd., Tokyo, Japan. From 1996 to 2000, he was a Research Fellow with the École Polytechnique de Montreal, Montreal, QC, Canada. From 2000 to 2013, he was an Associate Professor with the School of Electrical and Electronic Engineering, Nanyang Technological University, Singapore. He joined the Faculty of Science and Technology, University of Macau, Macau, China, as a Full Professor in August 2013, and has been a Distinguished Professor since December 2016. From August 2014 to August 2017, he served as the Head of Department of Electrical and Computer Engineering, University of Macau. So far, he has authored or coauthored more than 630 articles in international journals and conference proceedings. His articles have been cited more than 10.950 times with the H-index of 54 (source: Scopus). His research interests include microwave circuits, antennas, periodic structures, and computational electromagnetics.

Dr. Zhu served as the member for the IEEE MTT-S Fellow Evaluation Committee from 2013 to 2015 and the IEEE AP-S Fellows Committee from 2015 to 2017. He was the recipient of the 1997 Asia–Pacific Microwave Prize Award, the 1996 Silver Award of Excellent Invention from Matsushita-Kotobuki Electronics Industries Ltd., the 1993 Achievement Award in Science and Technology (first prize) from the National Education Committee of China, the 2020 FST Research Excellence Award from the University of Macau, and the 2020 Macao Natural Science Award (second prize) from the Science and Technology Development Fund (FDCT), Macau. He was the Associate Editors for the IEEE TRANSACTIONS ON MICROWAVE THEORY AND TECHNIQUES from 2010 to 2013 and the IEEE MICROWAVE AND WIRELESS COMPONENTS LETTERS from 2006 to 2012. He served as a General Chair for the 2008 IEEE MTT-S International Microwave Workshop Series on the Art of Miniaturizing RF and Microwave Passive Components, Chengdu, China, and a Technical Program Committee Co-Chair of the 2009 Asia–Pacific Microwave Conference, Singapore.

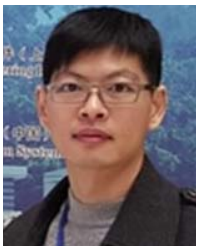

Sai-Wai Wong (Senior Member, IEEE) received the B.S. degree in electronic engineering from the Hong Kong University of Science and Technology, Hong Kong, in 2003, and the M.Sc. and Ph.D. degrees in communication engineering from Nanyang Technological University, Singapore, in 2006 and 2009, respectively.

From July 2003 to July 2005, he was an Electronic Engineer to lead the Electronic Engineering Department in China with two Hong Kong manufacturing companies. From May 2009 to October 2010, he was a Research Fellow with the ASTAR Institute for Infocomm Research, Singapore. Since 2010, he was an Associate Professor and later become a Full Professor, with the School of Electronic and Information Engineering, South China University of Technology, Guangzhou, China. From July 2016 to September 2016, he was a Visiting Professor with the City University of Hong Kong, Hong Kong. Since 2017, he has been a Full Professor with the College of Electronics and Information Engineering, Shenzhen University, Shenzhen, China. So far, he has authored and coauthored more than 200 articles in international journals and conference proceedings. His current research interests include RF/microwave circuit and antenna design.

Dr. Wong was the recipient of the New Century Excellent Talents in University awarded by the Ministry of Education of China in 2013 and the Shenzhen Overseas High-Caliber Personnel Level C in 2018.

Xu-Zhou Yu received the B.E. degree from the School of Electronic and Information Engineering, Tianjin University (TJU), Tianjin, China, in 2019. He is currently pursuing the master's degree with the College of Electronics and Information Engineering, Shenzhen University (SZU), Shenzhen, China.

His current research interest includes microwave cavity circuit design.

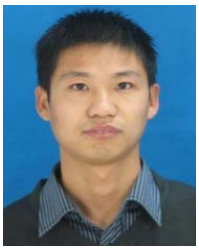

Yin Li (Member, IEEE) received the B.S. degree in applied physics from the China University of Petroleum, Dongying, China, in 2009, the M.Eng. degree in electromagnetic field and microwave technology from the University of Electronic Science and Technology of China (UESTC), Chengdu, China, in 2012, and the Ph.D. degree from the University of Macau, Macau, China.

From 2013 to 2015, he was a Research Assistant with the University of Hong Kong (HKU), Hong Kong. He is currently a Post-Doctoral Fellow with the School of Electronics and Information, Shenzhen University, Shenzhen, China. His current research interests include numerical modeling methods of passive microwave circuits, computational electromagnetics, and microwave circuits, frequency selectivity surface, and filtering antenna.

Wei He received the B.S. degree in electronic and information engineering from the Hunan University of Science and Technology, Xiangtan, Hunan, China, in 2010, and the M.S. degree in communication and information system from Shenzhen University, Shenzhen, China, in 2014, where he is currently pursuing the Ph.D. degree with the College of Electronics and Information Engineering.

His current research interests include RFID tag antennas, circularly polarized antennas and arrays, and metasurface.

Long Zhang (Member, IEEE) received the B.S. and M.S. degrees in electrical engineering from the Huazhong University of Science and Technology (HUST), Wuhan, China, in 2009 and 2012, respectively, and the Ph.D. degree in electronic engineering from the University of Kent, Canterbury, U.K, in 2017.

He was a Research Fellow with the Poly-Grames Research Center, Polytechnique Montreal, Montreal, QC, Canada. He is currently an Assistant Professor with the College of Electronics and Information Engineering, Shenzhen University, Shenzhen, China. His current research interests include circularly polarized antennas and arrays, mm-wave antennas and arrays, tightly coupled arrays, reflectarrays and characteristics mode theory.

Dr. Zhang served as a Reviewer for several technique journals, including the IEEE TRANSACTIONS ON ANTENNAS AND PROPAGATION, the IEEE ANTENNAS AND WIRELESS PROPAGATION LETTERS, the *IET Microwaves, Antennas & Propagation*, and the *Electronic Letters*.

Yejun He (Senior Member, IEEE) received the Ph.D. degree in information and communication engineering from the Huazhong University of Science and Technology (HUST), Wuhan, China, in 2005.

He has been a Full Professor with the College of Electronics and Information Engineering, Shenzhen University, Shenzhen, China, where he is the Director of Guangdong Engineering Research Center of Base Station Antennas and Propagation, and the Director of Shenzhen Key Laboratory of Antennas and Propagation, Shenzhen, China. He was selected as a Pengcheng Scholar Distinguished Professor, Shenzhen, China. He has authored or coauthored more than 200 research articles, books (chapters). He holds about 20 patents. His research interests include wireless communications, antennas and radio frequency.

Dr. He is a fellow of IET. He was also a recipient of the Shenzhen Overseas High-Caliber Personnel Level B (Peacock Plan Award B) and Shenzhen High-Level Professional Talent (Local Leading Talent). He received the 2016 Shenzhen Science and Technology Progress Award and the 2017 Guangdong Provincial Science and Technology Progress Award. He served as a General Chair for the IEEE ComComAp 2019. He is the Chair of the IEEE Antennas and Propagation Society-Shenzhen Chapter. He is serving as an Associate Editor for *IEEE Network* and *International Journal of Communication Systems and China Communications*.